Physics Letters A 380 (2016) 3570–3574

Contents lists available at ScienceDirect

Physics Letters A

www.elsevier.com/locate/pla

Self-induced light trapping in nonlinear Fabry–Perot resonators

K.N. Pichugin, A.F. Sadreev *

Kirensky Institute of Physics, 660036 Krasnoyarsk, Russia

ARTICLE INFO

Article history:
Received 13 June 2016
Received in revised form 12 August 2016
Accepted 13 August 2016
Available online 26 August 2016
Communicated by V.A. Markel

Keywords:
Bound state in the continuum
Nonlinear optics
Fabry–Perot resonator
Light storage

ABSTRACT

In the framework of the coupled mode theory we consider light trapping between two off-channel resonators which serve as self-adjusted Fano mirrors due to the Kerr effect. By inserting an auxiliary nonlinear resonator between the mirrors we achieve self-tuning of phase shift between the mirrors. That allows for the light trapping for arbitrary distance between the mirrors.

1. Introduction

One of the fundamental devices for trapping of light is a Fabry–Perot resonator with two Fano mirrors [1–4]. The simplest way to realize a Fano mirror in a photonic waveguide is to set up a side-coupled resonator demonstrated in Fig. 1 (a). In what follows we will refer to such side-coupled resonators as off-channel resonators. Then two paths of light, through the waveguide, and through the resonator, can interfere resulting in a full reflection at some definite frequency of light $\omega = \omega_0$ where ω_0 is the eigenfrequency of the resonator. Two such side-coupled resonators can act as a pair of perfect mirrors that trap waves between them. Thus, the structure formed by two Fano mirrors is equivalent to a Fabry–Perot resonator.

The light trapping is realized when the spacing L between the mirrors is tuned to make the round-trip phase shifts add up to an integer multiple of 2π to give rise to the Fabry–Perot bound state in the continuum (BSC) [5]. The BSCs in such structures were independently considered in application to different wave structures from quantum waveguide with two impurities [6], water waves between two obstacles [7], quantum transmission in temporally periodically driven potential wells [1], electron transport through double quantum dots [8–11] and photonic crystal structures [2–4, 12–17].

One important property of the BSC is resonant enhancement of the electromagnetic field as the resonance width tends to zero

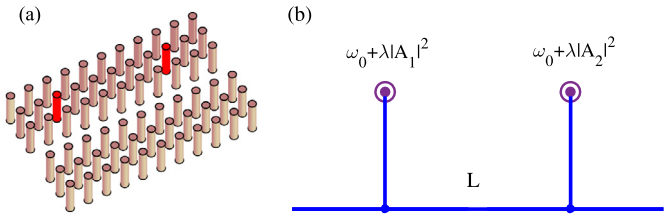

Fig. 1. (a) The photonic crystal structure, which consists of a square lattice of dielectric GaAs rods. Single row of rods is removed to form directional waveguide coupled to two off-channel single-mode resonators and (b) its coupled mode theory scheme.

[18–21]. Then nonlinear and optomechanical effects become important [22–28]. Remarkably, in this case the robust light trapping can be achieved without a necessity to tune material parameters of the system [23]. For the reader's convenience we illustrate the basic ideas behind this phenomenon by the example of the Fabry–Perot resonator composed of two identical nonlinear off-channel resonators side coupled with the linear waveguide [23] as depicted in Fig. 1.

In the linear case each off-channel resonator fully reflects light at the frequency $\omega = \omega_0$. Then if $k(\omega_0)L = \pi n, n = 1, 2, 3, \ldots$ the condition for standing waves between the Fano mirrors is fulfilled [3]. Therefore one has to tune both the distance L and the resonant frequency of the resonator ω_0 if the frequency of injected light is fixed. In the case of nonlinear resonators the resonant frequencies are shifted by the intensity of light in the resonator $\omega_0 + \lambda|A_j|^2, j = 1, 2$ due to the Kerr effect, where A_j are the amplitudes of resonant mode of the resonators. Then the condition for the Fano mirror $\omega = \omega_0 + \lambda|A_j|^2$ is satisfied without necessity

* Corresponding author.
E-mail addresses: knp@tnp.krasn.ru (K.N. Pichugin), almas@tnp.krasn.ru (A.F. Sadreev).

http://dx.doi.org/10.1016/j.physleta.2016.08.032
0375-9601/

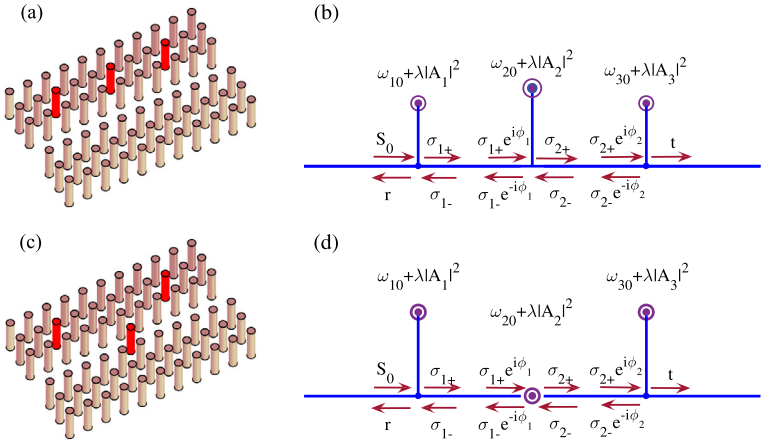

Fig. 2. The Fabry–Perot resonator with an auxiliary central nonlinear resonator side coupled with the waveguide (a) and (b) and the resonator in the waveguide (c) and (b).

to tune the material parameters or the frequency ω. However, we still have to adjust the distance between the mirrors.

In the present paper we show a possibility of stable light trapping in the nonlinear Fabry–Perot resonator without necessity to tune the resonant frequency of the Fano mirrors and the distance between them by implementation of an auxiliary nonlinear resonator as shown in Fig. 2. Such system can easily be considered in the framework of coupled mode theory [29,30].

2. Coupled mode theory of light trapping

Assume that we can neglect the dispersion of the photonic crystal waveguide: $k(\omega) = const$, and only a single eigenmode of each resonator resides in the propagation band of the waveguide. In general the auxiliary nonlinear resonator can be placed between the Fano mirrors non-symmetrically with different phase shifts between the left Fano mirror and the auxiliary resonator ϕ_1 and the right Fano mirror and the auxiliary resonator ϕ_2. We consider two cases for the auxiliary resonator: (a) side coupled with the waveguide and (b) in the waveguide.

2.1. Auxiliary resonator side-coupled with waveguide

The stationary CMT equations for the case of all three resonators side-coupled with the waveguide shown in Fig. 2 (a) and (b) take the following form [29,30]

$$\begin{aligned}
(\omega-\omega_1+i\Gamma)A_1 &= i\sqrt{\Gamma}(S_0+\sigma_{1-}),\\
(\omega-\omega_2+i\gamma)A_2 &= i\sqrt{\gamma}(\sigma_{1+}e^{i\phi_1}+\sigma_{2-}),\\
(\omega-\omega_3+i\Gamma)A_3 &= i\sqrt{\Gamma}\sigma_{2+}e^{i\phi_2},\\
\sigma_{1+} &= S_0-\sqrt{\Gamma}A_1,\\
S_{1-} &= \sigma_{1-}-\sqrt{\Gamma}A_1,\\
\sigma_{1-}e^{-i\phi_1} &= \sigma_{2-}-\sqrt{\gamma}A_2,\\
\sigma_{2+} &= \sigma_{1+}e^{i\phi_1}-\sqrt{\gamma}A_2,\\
t &= \sigma_{2+}e^{i\phi_2}-\sqrt{\Gamma}A_3,\\
\sigma_{2-}e^{-i\phi_2} &= -\sqrt{\Gamma}A_3.
\end{aligned} \tag{1}$$

Here A_j are the amplitudes of the resonant modes in resonators $j=1$ and $j=3$ and in the auxiliary resonator $j=2$; $\sigma_{j\pm}, r, t$ and S_0 are the amplitudes of waves in the sections of the waveguides as indicated in Fig. 2 (b); ϕ_1, ϕ_2 represent the phase shift incurred as the waveguide mode travels from the first Fano mirror to an auxiliary resonator and from the auxiliary resonator to the second Fano mirror; ω_j are the resonance frequencies of the resonators

$$\omega_j = \omega_{j0}+\lambda|A_j|^2, \tag{2}$$

$\sqrt{\Gamma}$ is the coupling of the resonators 1 and 3 and $\sqrt{\gamma}$ is the coupling of the auxiliary resonator with the waveguide, respectively. After simple algebra we can rewrite these equations as follows

$$\begin{aligned}
(\omega-\omega_1+i\Gamma)A_1+i\sqrt{\gamma\Gamma}e^{i\phi_1}A_2+i\Gamma e^{i(\phi_1+\phi_2)}A_3 &= i\sqrt{\Gamma}S_0,\\
i\sqrt{\gamma\Gamma}e^{i\phi_1}A_1+(\omega-\omega_2+i\gamma)A_2+i\sqrt{\gamma\Gamma}e^{i\phi_2}A_3 &= i\sqrt{\gamma}e^{i\phi_1}S_0,\\
i\Gamma e^{i(\phi_1+\phi_2)}A_1+i\sqrt{\gamma\Gamma}e^{i\phi_2}A_2+(\omega-\omega_3+i\Gamma)A_3 &\\
= i\sqrt{\Gamma}e^{i(\phi_1+\phi_2)}S_0, &\\
t = S_0e^{i(\phi_1+\phi_2)}-\sqrt{\Gamma}e^{i(\phi_1+\phi_2)}A_1-\sqrt{\gamma}e^{i\phi_2}A_2-\sqrt{\Gamma}A_3, &\\
r = S_{1-} = -\sqrt{\Gamma}A_1-\sqrt{\gamma}e^{i\phi_1}A_2-\sqrt{\Gamma}e^{i(\phi_1+\phi_2)}A_3. &
\end{aligned} \tag{3}$$

The first three equations for mode amplitudes A_j, $j=1,2,3$ can be written in the compact form

$$(\omega-\hat{H}_{\text{eff}})\mathbf{A} = \mathbf{\Psi}_{\text{in}} \tag{4}$$

and can be interpreted as the Lippmann–Schwinger equation [2,4] with the non Hermitian Hamiltonian

$$\hat{H}_{\text{eff}} = \begin{pmatrix} \omega_1-i\Gamma & -i\sqrt{\gamma\Gamma}e^{i\phi_1} & -i\Gamma e^{i(\phi_1+\phi_2)} \\ -i\sqrt{\gamma\Gamma}e^{i\phi_1} & \omega_2-i\gamma & -i\sqrt{\gamma\Gamma}e^{i\phi_2} \\ -i\Gamma e^{i(\phi_1+\phi_2)} & -i\sqrt{\gamma\Gamma}e^{i\phi_2} & \omega_3-i\Gamma \end{pmatrix}, \tag{5}$$

and

$$\mathbf{\Psi}_{\text{in}} = iS_0\begin{pmatrix} \sqrt{\Gamma} \\ \sqrt{\gamma}e^{i\phi_1} \\ \sqrt{\Gamma}e^{i(\phi_1+\phi_2)} \end{pmatrix}. \tag{6}$$

The solution of Eq. (4) is given by the inverse of the matrix $(\omega-\hat{H}_{eff})$. However, there could be a case that the inverse matrix does not exist, i.e., the determinant of the matrix equals zero. The condition for BSC is given by equation

$$||\omega_c-\hat{H}_{\text{eff}}|| = 0, \tag{7}$$

where ω_c is the discrete eigenfrequency of the BSC. This equation with account of Eq. (2) gives the following equalities

$$\begin{aligned}
\omega_c &= \omega_{10}+\lambda|A_{1c}|^2 = \omega_{30}+\lambda|A_{3c}|^2, \quad |A_{1c}| = |A_{3c}|,\\
\omega_c &= \omega_2+\lambda|A_{2c}|^2-\frac{2\gamma}{\cot\phi_1+\cot\phi_2}.
\end{aligned} \tag{8}$$

The first equality in this equation defines the condition of the self-adjusted Fano mirror [23] while the second equality gives us the

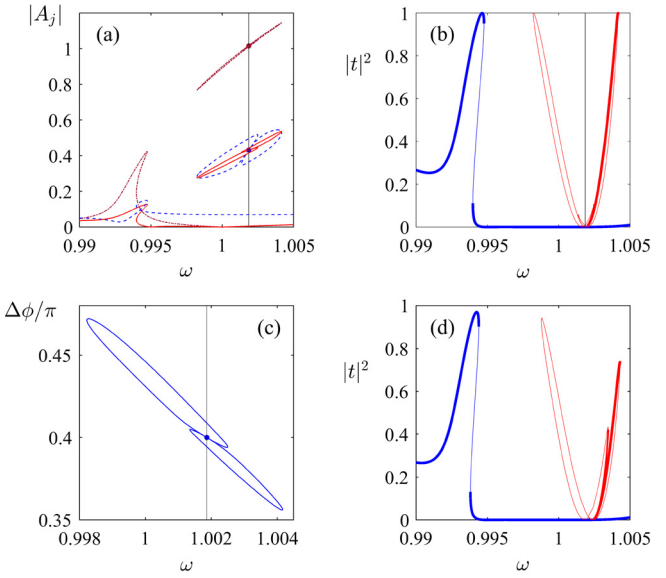

Fig. 3. Frequency dependence of the resonator amplitudes $|A_j|$ (a), transmittance $|t|^2$ (b) and phase difference (c) calculated for the parameters $\Gamma = 0.01, \gamma = 0.0025, \phi_1 = \phi_2 = 0.3\pi, \lambda = 0.01, \omega_{10} = \omega_{30} = 1, \omega_{20} = 0.995, S_0 = 0.007$. The BSC point is marked by closed circle. The mode amplitudes A_j are shown in (a) by blue dash ($j = 1$), brown dash–dot ($j = 2$), and red solid ($j = 3$) lines. (d) The case of non-symmetrical position of the auxiliary in-channel resonator with $\phi_1 = 0.3\pi, \phi_2 = 0.35\pi$. Thin vertical line shows the BSC frequency (8). Thicker lines in the transmittance mark stable parts of the solutions. (For interpretation of the references to color in this figure legend, the reader is referred to the web version of this article.)

condition for the self-tuning of phase shift between the Fano mirrors. Substitution of this equation into Eq. (4) for $\Psi_{in} = 0$ gives additional equations for the BSC amplitudes

$$A_{1c}\sin\phi_1 = A_{3c}\sin\phi_2,$$
$$A_{2c} = -\sqrt{\frac{\Gamma}{\gamma}}(A_{1c}\cos\phi_1 + A_{3c}\cos\phi_2). \tag{9}$$

Because the intensities at the Fano mirrors have to be equal we immediately obtain that $\omega_{10} = \omega_{30}$ and the auxiliary resonator has to be placed symmetrically between the mirrors: $\phi_1 = \phi_2 = \phi$. Then we get the following equalities for the BSC intensities

$$\lambda|A_{1c}|^2 = \lambda|A_{3c}|^2 = \frac{\omega_{20} - \omega_{10} - \gamma\tan\phi}{1 - \frac{4\Gamma}{\gamma}\cos^2\phi},$$
$$|A_{2c}|^2 = \frac{4\Gamma}{\gamma}\cos^2\phi|A_{1c}|^2. \tag{10}$$

Numerical solutions of nonlinear equations (3) and (7) shown in Fig. 3 demonstrate two different solutions. The first solution inherited from the linear case shows a typical excitation of the resonators whose mode amplitudes shown in Fig. 3 (a) tends to zero when the injected amplitude $S_0 \to 0$. Respectively this solution gives transmission zeros as shown in Fig. 3 (b). Due to three resonators side coupled with the waveguide these zeros coalesce to give rise to wide domain in frequency $0.995 \le \omega \le 1.005$ where the system almost perfectly reflects light.

Besides there is a solution for the resonator mode amplitudes A_j which has a shape of closed loops in Fig. 3 (a) which shrink to the BSC points given by Eqs. (8), (9) and (10) when $S_0 \to 0$. In what follows we term this solution as the BSC originated solution although the BSC is corrupted with the growth of injected power [23]. This solution contributes into the transmittance in the form of a butterfly shape resonance as shown in Fig. 3 (b). Again as the injected power is decreased the width of the resonance tends to zero.

Fig. 3 (c) demonstrates the behavior of the phase difference $\Delta\phi = arg(\sigma_R) - arg(\sigma_L)$ between the waveguide modes ingoing and outgoing to the auxiliary resonator. Here $\sigma_R = \sigma_{2+}, \sigma_L = \sigma_{1+}e^{i\phi_1}$. The phase shift incurred as the waveguide mode travels from the first Fano mirror to the second mirror was chosen 0.6π. As Fig. 3 (c) demonstrates the auxiliary resonator provides the phase shift 0.4π at the BSC point to give rise to the total phase shift π. Thus one can see that nonlinearity of the off-channel auxiliary resonator lifts the necessity to adjust the distance between the mirrors provided that the phase ϕ belongs to the domain where the intensities $|A_{jc}|^2$ defined by Eq. (10) remains positive.

The stability of the solutions was inspected by standard methods of small perturbations [31]. The stability domains are marked by lines thicker in the transmittance (Fig. 3 (b)). It is surprising that fingerprints of the BSC are seen even when the auxiliary resonator is placed between the Fano mirrors non-symmetrically, i.e., when $\phi_1 \neq \phi_2$ as shown in Fig. 3 (d).

2.2. Auxiliary resonator in the waveguide

The case is shown in Fig. 2 (c) and (d). The coupled mode theory equations coincide with Eqs. (1) except the equations for light flows through the auxiliary in waveguide resonator for $\phi_1 = \phi_2$ [29, 30]:

$$\sigma_{1-}e^{-i\phi} = -\sigma_{1+}e^{i\phi} + \sqrt{\gamma}A_2,$$
$$\sigma_{2+} = -\sigma_{2-} + \sqrt{\gamma}A_2. \tag{11}$$

As a result we have the following equations for the amplitudes A_j:

$$[\omega - \omega_1 + i\Gamma(1 - e^{2i\phi})]A_1 - i\sqrt{\gamma\Gamma}e^{i\phi}A_2 = i\sqrt{\Gamma}S_0(1 - e^{2i\phi}),$$
$$i\sqrt{\gamma\Gamma}e^{i\phi}A_1 + (\omega - \omega_2 + i\gamma)A_2 + i\sqrt{\gamma\Gamma}e^{i\phi}A_3 = i\sqrt{\gamma}e^{i\phi}S_0,$$
$$-i\sqrt{\gamma\Gamma}e^{i\phi}A_2 + [\omega - \omega_3 + i\Gamma(1 - e^{2i\phi})]A_3 = 0,$$
$$t = \sqrt{\Gamma}(e^{2i\phi} - 1)A_3 + \sqrt{\gamma}e^{i\phi}A_2,$$
$$r = S_{1-} = -S_0e^{2i\phi} + \sqrt{\Gamma}(e^{2i\phi} - 1)A_1 + \sqrt{\gamma}e^{i\phi}A_2. \tag{12}$$

Repeating calculations described in subsection A we obtain equations similar to Eqs. (8)–(10) except that $\phi \to \phi + \pi/2$:

$$\lambda|A_{1c}|^2 = \lambda|A_{3c}|^2 = \frac{\omega_{20} - \omega_{10} + \gamma\cot\phi}{1 - \frac{4\Gamma}{\gamma}\sin^2\phi},$$
$$|A_{2c}|^2 = \frac{4\Gamma}{\gamma}|A_{1c}|^2\sin^2\phi. \tag{13}$$

with the BSC frequency

$$\omega_c = \omega_{10} + \lambda|A_{1c}|^2. \tag{14}$$

As seen from Fig. 4 the frequency dependence of the BSC originated solution induced butterfly type resonance is very similar to the previous case of auxiliary resonator side coupled with the waveguide shown in Fig. 3.

3. Light storage in Fabry–Perot BSC

Following Ref. [27] we consider the trapping of a Gaussian pulse by a Fabry–Perot BSC, i.e. the effect of light storage. The mechanism of the light storage by the BSCs is the following. Assume for a moment that the amplitude of the injected wave is so small that we can neglect the nonlinearity. Because the BSC is completely decoupled from the continuum in a linear system it can not be probed by the incoming wave. However, with the increase of the

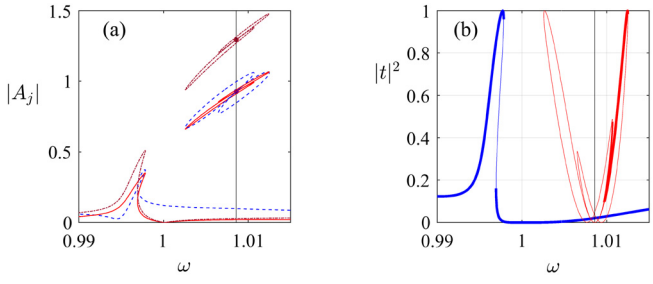

Fig. 4. Frequency dependence of the amplitudes $|A_j|$ (a) and transmittance $|t|^2$ (b) for the case of auxiliary nonlinear resonator in the waveguide with the parameters $\Gamma = 0.01, \gamma = 0.02, \phi = 0.55\pi, \lambda = 0.01, \omega_{10} = \omega_{30} = 1, \omega_{20} = 0.995, S_0 = 0.012$. The BSC point given by Eqs. (13) and (14) is marked by closed circle. Thicker lines in the transmittance mark stable parts of the solutions.

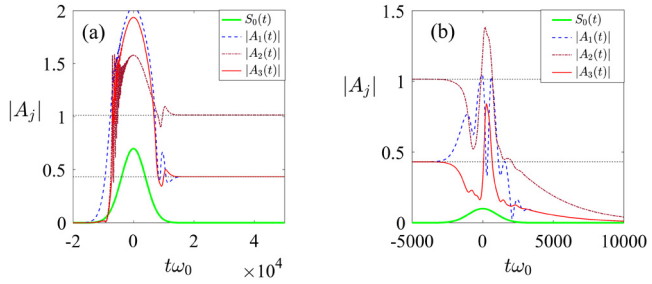

Fig. 5. (Color online.) Time evolution by Eqs. (17) of mode amplitudes $|A_1|$ (blue dashed line), $|A_2|$ (brown dash–dot line) and $|A_3|$ (red solid line) after the injection of a first gaussian pulse shown by thick green solid line with $\sigma = 4000, E_0 = 0.7$ (a) and a secondary pulse with $\sigma = 1000, E_0 = 0.1$. The parameters of the system is given in Fig. 3 caption. Horizontal black dash lines show the BSC amplitude given by Eqs. (10).

injected power the Kerr effect of the resonators becomes important killing two birds with one stone. First, there is no necessity for tuning material parameters because the Kerr effect in the resonators results in occurrence of self-induced BSCs as was shown in previous sections. Second, the nonlinearity couples the BSC with the continuum so that the injected wave excites the BSC transforming it into a quasi-BSC [22,23]. Once the pulse has passed by the Fabry–Perot resonator the quasi-BSC is again decoupled from the waveguide and becomes a true BSC. As a result some amount of light is trapped in the true BSC opening an opportunity for light storage. Finally, the application of a secondary pulse again transforms the true BSC into a quasi-BSC with finite life-time and completely releases the light. In this section we apply these ideas on the present Fabry–Perot resonator.

The time dependent coupled mode theory equations for off-channel resonator have the following form [2,3]

$$i\dot{\mathbf{A}}(t) = \hat{H}_{\text{eff}}\mathbf{A}(t) + \mathbf{\Psi}_{\text{in}}(t)e^{-i\omega t} \tag{15}$$

where $\hat{H}_{\text{eff}}$ is effective Hamiltonian (5), $\mathbf{\Psi}_{\text{in}}$ is incoming wave (6) with

$$S_0(t) = E_0 \exp(-t^2/2\sigma^2). \tag{16}$$

For a monochromatic wave $\phi = k(\omega)L$. However for a light pulse which is an expansion over monochromatic waves these equations (15) are not valid. Therefore we have to modify Eqs. (15) taking into consideration the delay time $\tau = \phi/\omega$ for travelling from one resonator to another [27]

$$\begin{aligned}
i\dot{A}_1 &= (\omega_{10} + \lambda|A_1|^2 - i\Gamma)A_1(t) - i\sqrt{\gamma\Gamma}A_2(t-\tau) \\
&\quad -i\Gamma A_3(t-2\tau) + i\sqrt{\Gamma}S_0(t)e^{-i\omega t}, \\
i\dot{A}_2 &= (\omega_{20} + \lambda|A_2|^2 - i\gamma)A_2(t) - i\sqrt{\gamma\Gamma}A_1(t-\tau) \\
&\quad -i\Gamma A_3(t-\tau) + i\sqrt{\gamma}S_0(t-\tau)e^{-i\omega(t-\tau)}, \\
i\dot{A}_3 &= (\omega_{30} + \lambda|A_3|^2 - i\Gamma)A_3(t) - i\sqrt{\gamma\Gamma}A_2(t-\tau) \\
&\quad -i\Gamma A_1(t-2\tau) + i\sqrt{\Gamma}S_0(t-2\tau)e^{-i\omega(t-2\tau)}.
\end{aligned} \tag{17}$$

Numerical integration give us solution of these equations presented in Fig. 5.

In Fig. 5 (a) one can see that the effect of light trapping is achieved without tuning the parameters. One can also see from Fig. 5 (b) that the injection of a secondary pulse can release the trapped light from the BSC paving a way for self-adjusting all-optical light storage devices.

4. Conclusions

In the framework of the stationary coupled mode theory we revealed two important conceptual aspects of light trapping in Fabry–Perot systems with account of the Kerr effect. The first aspect is related to a self-adjusted Fano mirror based on the off-channel resonator with the eigenfrequency ω_0 [32]. For any frequency ω of injected light such mirror is capable for perfect reflection due to the Kerr shift of the eigenfrequency of the resonator $\omega = \omega_0 + \lambda|A|^2$ where A is the amplitude of eigenmode. Thus, exploiting two identical nonlinear Fano mirrors one can design a Fabry–Perot resonator which can support self-induced BSCs [23]. However, the distance between the mirrors L has to be adjusted for holding an integer number of half wavelengths $\phi = kL = \pi n, n = 1, 2, 3, \ldots$. The second aspect is related to a self-tuning of phase shift between the Fano mirrors due to nonlinear response of an auxiliary resonator placed between the mirrors. That relaxes the necessity to tune a distance between the mirrors. The third aspect important with experimental view of point is the effect of light absorption. The light absorption quantitatively given by the quality factor Q transforms the true BSC into the quasi-BSC with the life time proportional to Q. Respectively the amplitudes A_j in Fig. 5 will decay after this time. We analyzed the stability of the solutions to reveal that only fragments of the BSC originated solution are stable while the solution inherited from the linear case is stable for all frequencies. Nevertheless we speculate it is sufficient to observe the trapped BSC solution as a response, for example, to injected laser pulses.

Acknowledgements

We thank D.N. Maksimov for discussions. The work was supported by Russian Science Foundation through grant 14-12-00266.

References

[1] C.S. Kim, A.M. Satanin, Coherent resonant transmission in temporally periodically driven potential wells: the Fano mirror, J. Phys. Condens. Matter 10 (47) (1998) 10587–10598, http://dx.doi.org/10.1088/0953-8984/10/47/010.
[2] S. Fan, P. Villeneuve, J. Joannopoulos, M. Khan, C. Manolatou, H. Haus, Theoretical analysis of channel drop tunneling processes, Phys. Rev. B 59 (24) (1999) 15882–15892, http://dx.doi.org/10.1103/PhysRevB.59.15882.
[3] Z. Wang, S. Fan, Compact all-pass filters in photonic crystals as the building block for high-capacity optical delay lines, Phys. Rev. E 68 (6) (2003) 066616, http://dx.doi.org/10.1103/PhysRevE.68.066616.
[4] E. Bulgakov, A. Sadreev, Bound states in the continuum in photonic waveguides inspired by defects, Phys. Rev. B 78 (7) (2008) 075105, http://dx.doi.org/10.1103/PhysRevB.78.075105.
[5] C.W. Hsu, B. Zhen, A.D. Stone, J.D. Joannopoulos, M. Soljačić, Bound states in the continuum, Nat. Rev. Mater. 1 (2016) 16048, http://dx.doi.org/10.1038/natrevmats.2016.48.
[6] T.V. Shahbazyan, M.E. Raikh, Two-channel resonant tunneling, Phys. Rev. B 49 (24) (1994) 17123–17129, http://dx.doi.org/10.1103/physrevb.49.17123.
[7] M. McIver, An example of non-uniqueness in the two-dimensional linear water wave problem, J. Fluid Mech. 315 (1) (1996) 257, http://dx.doi.org/10.1017/s0022112096002418.

[8] I. Rotter, A.F. Sadreev, Zeros in single-channel transmission through double quantum dots, Phys. Rev. E 71 (4) (2005) 046204, http://dx.doi.org/10.1103/physreve.71.046204.
[9] A.F. Sadreev, E.N. Bulgakov, I. Rotter, S-matrix formalism of transmission through two quantum billiards coupled by a waveguide, J. Phys. A, Math. Gen. 38 (49) (2005) 10647–10661, http://dx.doi.org/10.1088/0305-4470/38/49/012.
[10] G. Ordonez, K. Na, S. Kim, Bound states in the continuum in quantum-dot pairs, Phys. Rev. A 73 (2) (2006) 022113, http://dx.doi.org/10.1103/physreva.73.022113.
[11] J.-W. Liaw, C.-H. Huang, B.-R. Chen, M.-K. Kuo, Subwavelength Fabry–Perot resonator: a pair of quantum dots incorporated with gold nanorod, Nanoscale Res. Lett. 7 (1) (2012) 546, http://dx.doi.org/10.1186/1556-276x-7-546.
[12] L.-L. Lin, Z.-Y. Li, B. Lin, Engineering waveguide-cavity resonant side coupling in a dynamically tunable ultracompact photonic crystal filter, Phys. Rev. B 72 (16) (2005) 165330, http://dx.doi.org/10.1103/physrevb.72.165330.
[13] D. Marinica, A. Borisov, S. Shabanov, Bound states in the continuum in photonics, Phys. Rev. Lett. 100 (18) (2008) 183902, http://dx.doi.org/10.1103/PhysRevLett.100.183902.
[14] R.F. Ndangali, S.V. Shabanov, Electromagnetic bound states in the radiation continuum for periodic double arrays of subwavelength dielectric cylinders, J. Math. Phys. 51 (10) (2010) 102901, http://dx.doi.org/10.1063/1.3486358.
[15] C.W. Hsu, B. Zhen, J. Lee, S.-L. Chua, S.G. Johnson, J.D. Joannopoulos, M. Soljačić, Observation of trapped light within the radiation continuum, Nature 499 (7457) (2013) 188–191, http://dx.doi.org/10.1038/nature12289.
[16] B. Zhen, C.W. Hsu, L. Lu, A.D. Stone, M. Soljačić, Topological nature of optical bound states in the continuum, Phys. Rev. Lett. 113 (25) (2014) 257401, http://dx.doi.org/10.1103/physrevlett.113.257401.
[17] L. Li, H. Yin, Bound states in the continuum in double layer structures, Sci. Rep. 6 (2016) 26988, http://dx.doi.org/10.1038/srep26988.
[18] A. Sadreev, E. Bulgakov, I. Rotter, Bound states in the continuum in open quantum billiards with a variable shape, Phys. Rev. B 73 (23) (2006) 235342, http://dx.doi.org/10.1103/PhysRevB.73.235342.
[19] M. Zhang, X. Zhang, Ultrasensitive optical absorption in graphene based on bound states in the continuum, Sci. Rep. 5 (2015) 8266, http://dx.doi.org/10.1038/srep08266.
[20] V. Mocella, S. Romano, Giant field enhancement in photonic resonant lattices, Phys. Rev. B 92 (15) (2015) 155117, http://dx.doi.org/10.1103/physrevb.92.155117.
[21] M. Song, H. Yu, C. Wang, N. Yao, M. Pu, J. Luo, Z. Zhang, X. Luo, Sharp Fano resonance induced by a single layer of nanorods with perturbed periodicity, Opt. Express 23 (3) (2015) 2895–2903, http://dx.doi.org/10.1364/oe.23.002895.
[22] E. Bulgakov, A. Sadreev, Resonance induced by a bound state in the continuum in a two-level nonlinear Fano–Anderson model, Phys. Rev. B 80 (11) (2009) 115308, http://dx.doi.org/10.1103/PhysRevB.80.115308.
[23] E.N. Bulgakov, A.F. Sadreev, Bound states in photonic Fabry–Perot resonator with nonlinear off-channel defects, Phys. Rev. B 81 (11) (2010) 115128, http://dx.doi.org/10.1103/PhysRevB.81.115128.
[24] M. Molina, A. Miroshnichenko, Y. Kivshar, Surface bound states in the continuum, Phys. Rev. Lett. 108 (7) (2012) 070401, http://dx.doi.org/10.1103/PhysRevLett.108.070401.
[25] S. Longhi, G. Della Valle, Many-particle quantum decay and trapping: the role of statistics and Fano resonances, Phys. Rev. A 86 (1) (2012) 012112, http://dx.doi.org/10.1103/physreva.86.012112.
[26] E.N. Bulgakov, A.F. Sadreev, Robust bound state in the continuum in a nonlinear microcavity embedded in a photonic crystal waveguide, Opt. Lett. 39 (17) (2014) 5212–5215, http://dx.doi.org/10.1364/ol.39.005212.
[27] E.N. Bulgakov, K.N. Pichugin, A.F. Sadreev, All-optical light storage in bound states in the continuum and release by demand, Opt. Express 23 (17) (2015) 22520, http://dx.doi.org/10.1364/oe.23.022520.
[28] L. Yuan, Y.Y. Lu, Diffraction of plane waves by a periodic array of nonlinear circular cylinders, Phys. Rev. A 94 (1) (2016) 013852, http://dx.doi.org/10.1103/physreva.94.013852.
[29] S. Fan, W. Suh, J.D. Joannopoulos, Temporal coupled-mode theory for the Fano resonance in optical resonators, J. Opt. Soc. Am. A 20 (3) (2003) 569–572, http://dx.doi.org/10.1364/josaa.20.000569.
[30] W. Suh, Z. Wang, S. Fan, Temporal coupled-mode theory and the presence of non-orthogonal modes in lossless multimode cavities, IEEE J. Quantum Electron. 40 (10) (2004) 1511–1518, http://dx.doi.org/10.1109/jqe.2004.834773.
[31] A.R. Cowan, J.F. Young, Optical bistability involving photonic crystal microcavities and Fano line shapes, Phys. Rev. E 68 (4) (2003) 046606, http://dx.doi.org/10.1103/physreve.68.046606.
[32] A.E. Miroshnichenko, S.F. Mingaleev, S. Flach, Y.S. Kivshar, Nonlinear Fano resonance and bistable wave transmission, Phys. Rev. E 71 (3) (2005) 036626, http://dx.doi.org/10.1103/physreve.71.036626.